Nonlinear Dynamics of Semiconductor Laser Emission Under Variable Feedback Conditions

Joachim Sacher, Wolfgang Elsässer, and Ernst O. Göbel

Abstract—**We have studied the behavior of external cavity semiconductor lasers with tilted external cavity mirrors providing variable feedback. We demonstate the appearance of intermittent breakdowns of the light intensity induced by the tilting of the external mirror. The rate of the breakdowns of the light intensity is directly related to the relaxation oscillation frequency of the external cavity semiconductor laser. We are able to describe the experimental observations theoretically by the coupled rate equations for the electric field density and the carrier density.**

I. Introduction

THE optical properties of semiconductor lasers with external feedback are of profound interest because of the practical importance as well as the basic properties of this nonlinear system. External cavity semiconductor lasers, for instance, are used for linewidth reduction [1] or short pulse generation [2]. Semiconductor lasers with external feedback, however, have also received considerable attention for the investigations of optical chaos [3]–[9]. In particular two of the universal transitions to chaos have been found: the quasi-periodic [8] and the intermittency route [9]. The quasi-periodic route is observed in external cavity semiconductor lasers with an increase of the feedback level from zero to strong feedback. The intermittency route has been demonstrated in the case of strong feedback in the regime of the coherence collapse [9], i.e., at an injection current corresponding to the laser threshold without feedback.

The behavior of the external cavity semiconductor laser is theoretically described by the coupled rate equations for the electric field and the carrier density. The laser with delayed feedback due to the external cavity mirror represents a system with infinite dimension according to its mathematic description [10]. However, there are only a finite number of dimensions excited [5], [11]. This number of the excited degrees of freedom is determined by the system parameters as well as by the feedback conditions.

In this paper we report the influence of the feedback conditions on the optical output of the semiconductor laser. We demonstrate the occurence of an intermittent transition from the stable regime to a regular self-pulsating operation. The system is in a stable region of operation for optimum adjustment of the external cavity mirror. The feedback under optimum alignment is the highest. The injection current is chosen to be below the coherence collapse [9]. The optical output of the laser system becomes unstable by tilting the external cavity mirror. First, for small tilting angles of the external cavity mirror we observe intermittent behavior in the light intensity, which corresponds to a breakup of the regular torus describing the system in phase space. This is accompanied with an increase of the required dimensionality of the phase space. Further tilting of the mirror leads to regular self-pulsations [12]. We demonstrate that the frequency of these self-pulsations reflects the coupled light intensity—carrier density—oscillations, i.e., the relaxation oscillations.

The paper is structured as føllows. After this introduction we shall now describe the experimental setup and the experimental observations in Section II. In Section III we present the theoretical model and in Section IV we compare the model calculations with our experimental results.

Manuscript received July 2, 1990; revised November 5, 1990. This work was supported by the Deutsche Forschungsgemeinschaft within the Sonderforschungsbereich 185 (Nichtlineare Dynamik).

The authors are with the Fachbereich Physik der Philipps-Universität Marburg, D-3550 Marburg, Germany.

IEEE Log Number 9143042.

II. Experimental

The experimental setup is shown in Fig. 1. We use a temperature-stabilized GaAs–GaAlAs channeled substrate planar semiconductor laser (HLP1400, denoted as LD in Fig. 1). The external cavity (on the right-hand side of the LD) consists of an antireflection coated microscope objective to collimate the laser beam and a high-reflecting dielectric mirror (98%), which is revolvable in the horizontal and vertical direction. The detection part is on the left-hand side of the LD. The optical spectrum of the semiconductor laser is measured using a 1 m Czerny–Turner grating monochromator and a scanning plane Fabry–Perot interferometer. The time-averaged laser light intensity is measured by a slow p–i–n diode. The fast fluctuations are detected by an avalanche photodiode (APD, risetime ≤ 100 ps). Its electrical output is amplified and then analyzed in the frequency and in the time domain using a RF spectrum analyzer and a transient digitizer (bandwidth 600 MHz), respectively.

We achieve a threshold reduction of 9.2% from 52.4 mA down to 47.6 mA under optimal feedback conditions (optimum external mirror alignment). The injection current is kept at 51.6 mA through the measurements, which is below 52.4 mA where the coherence collapse value occurs [9]. In the present studies the feedback is varied by tilting the external cavity mirror in horizontal as well as in vertical direction. Therefore we have a two-dimensional parameter space.

Tilting of the mirror has a pronounced influence on the time-averaged optical output power of the laser. The dependence of the laser intensity on horizontal and vertical mirror tiltings is depicted in Fig. 2(a). The contour plot depicted in Fig. 2(b) is calculated from the data set of Fig. 2(a). The case of optimal feedback conditions no tilting of the external cavity mirror) cor-

0018-9197/91/0300-0373$01.00 © 1991 IEEE

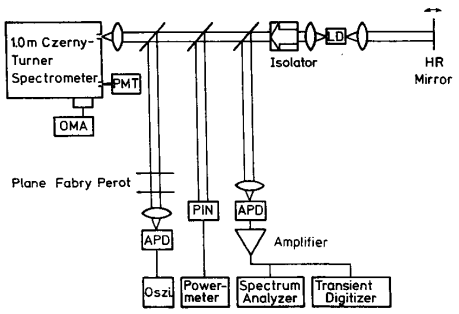

Fig. 1. The experimental setup consisting of the feedback part on the RHS of the semiconductor laser (LD) and the detection part on the LHS.

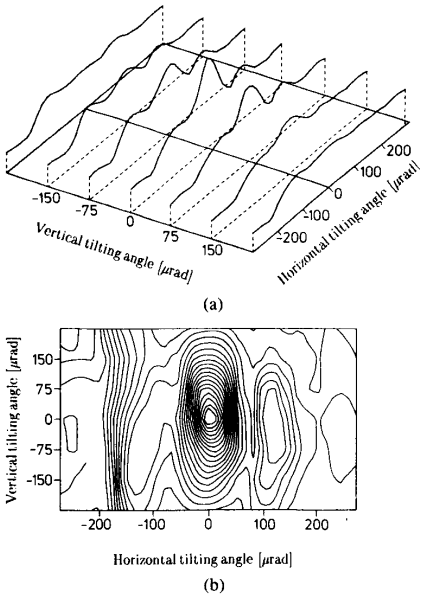

Fig. 2. The time averaged light intensity is shown versus the horizontal and vertical mirror tilting angle. Part (a) shows the experimental data in a three-dimensional plot. The dashed curves indicate the mirror angle. Part (b) shows a contour plot of the experimental data.

responds to the maximum of the light intensity. This point is chosen to define the zero point of the tilting angles in horizontal as well as vertical directions. Starting from this zero point and tilting the mirror in the horizontal direction, the light intensity decreases until it reaches a minimum value at an angle of 79 μrad. The light intensity increases again with further increase of the tilting angle until a side maximum is reached at an angle of 117 μrad. This pronounced side maximum does not appear for vertical tilting. For negative tilting angles in horizontal as well as vertical direction, the light intensity behavior is quite similar. Complementary to this characteristic behavior of the time-averaged light intensity of the external cavity semiconductor laser, we also observe characteristic transitions in the fast fluctuations of the laser light.

With an increasing tilting angle of the external cavity mirror, the laser output starts from stable operation at the zero point, then passes an intermittent regime, and finally shows regular self-pulsations. These transitions are summarized in detail by the data in Fig. 3, where the laser output is characterized by the power spectrum (left column), by single-shot traces of the time signal (center column), and by two-dimensional projections of the attractor (right column). The external mirror tilting in the horizontal direction amounts to 0 μrad in Fig. 3(a), 4 μrad in Fig. 3(b), 8 μrad in Fig. 3(c), and 17 μrad in Fig. 3(d), respectively.

The behavior of the laser output can be classified in five different regimes according to the dependence of the fast fluctuations of the laser light on the tilting angle of the external cavity mirror and the dependence of the time-averaged light intensity of the laser on the tilting angle: 1) regular external cavity multimode laser, 2) intermittency in the light intensity, 3) external cavity relaxation oscillations and frequency locking, 4) side maximum, and 5) double round-trip. They will discussed in more detail below for the case of horizontal (Section II-A) and for the case of vertical mirror tilting (Section II-B).

A) Horizontal Tilting of the External Cavity Mirror

On the base of the general overview presented so far we begin with the detailed discussion of the five different operation regions. Therefore, we start at the point of maximum output power (zero point) and then the mirror is tilted in the horizontal direction. The discussion will be completed in (Section II-B) describing the behavior under vertical tilting of the external cavity mirror.

1) Regular External Cavity Multimode Laser: We start with a description of the system for optimum feedback. This case is depicted in Fig. 3(a). The left part of Fig. 3(a) shows the power spectrum. The peak at 352 MHz in the power spectrum corresponds to the beat frequency of the external cavity frequencies. This frequency f_R is determined by the length L of the external cavity according to $f_R = c/2L$. The origin of the broad peak shifted by 29 MHz to a higher frequency is not completely understood, however, this peak will not be considered in the present paper. The middle part of Fig. 3(a) shows the observed time signal. The trace is nearly flat because the external cavity oscillation period (2.5 ns) is not resolved on this time scale. The two-dimensional projection of the phase space in the RHS of Fig. 3(a) is reconstructed by the data set of the time signal. The projection is a fixed point as expected by the stable time signal.

2) Intermittency in the Light Intensity: The intermittency in the light output is observed for small tilting angles of the external cavity mirror. This small tilting (typically of the order of 4–30 μrad) causes a change in the feedback geometry of the external cavity laser. This means that the light reflected back to the laser facet facing the external mirror is not coupled exactly into the active region of the semiconductor laser. Therefore the coupling between the laser and the external cavity is reduced and the output power decreases. However, the system is not in a stable regime and the laser output shows pronounced fluctuations. In Fig. 3(b) we depict the experimental results for a horizontal tilting angle of 4 μrad. We observe the appearance of low frequency noise in the power spectrum [LHS of Fig. 3(b)] and simultaneously a weak line broadening of the external cavity beat frequency. The time signal [middle part of Fig. 3(b)] shows statistically distributed breakdowns. These breakdowns are the origin of the low frequency noise in the power spectrum as confirmed by a Fourier transformation of the experimental time signal data. The RHS of Fig. 3(b) depicts the corresponding projection of the phase space. We recognize the breakup of

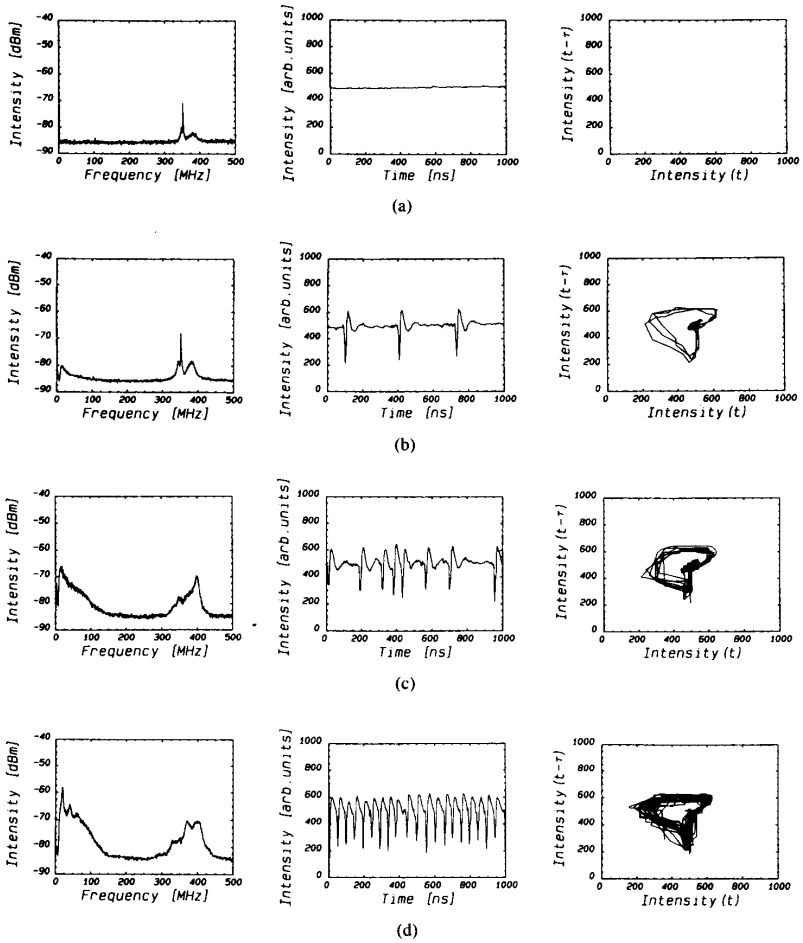

Fig. 3. Power spectra (left column), time signal (central column), and two-dimensional attractor projection (right column) of the optical output power of the laser. From the top to the bottom the different lines correspond to a tilting angle of (a) 0 μrad, (b) 4 μrad, (c) 8 μrad, (d) 17 μrad. The power spectrum and the time signal in one line are simultaneously measured. The attractor projection is reconstructed by the delay time method of Takens. The delay time of all projections amounts to 7.81 ns.

the fix-point attractor of Fig. 3(a) by intermitting events. However, the attractor describing the system is restricted to a limited area in the phase space as seen in the right column of Fig. 3. In addition to the occurence of intermittency we would like to point out that after the breakdown the laser emission relaxes into its stationary value with a characteristic oscillation behavior [middle part of Fig. 3(b)]. A further increase of the tilting angle of the external cavity mirror results in an enhanced occurence of the breakdown events. This leads to an interesting phenomena at a mirror angle of 8 μrad where both the breakdown rate and the characteristic oscillation frequency coincide. As seen in the middle part of Fig. 3(c) the behavior of the light intensity is determined by the breakdown rate instead of exhibiting a relaxation oscillation process. This means that the characteristic relaxation oscillation process will be a limitation of the breakdown rate as seen in the middle part of Fig. 3(d) which corresponds to an even larger tilting angle of 17 μrad. Under this condition of strong tilting, the power spectrum [LHS of Fig. 3(d)] exhibits a structured low-frequency noise corresponding to the relaxation process. With a further increase of the mirror angle these sharp frequencies will become even more pronounced. Obviously, a relation between the breakdowns and the characteristic relaxation oscillations exists. In the following we will show that the characteristic oscillations correspond to the intrinsic relaxation oscillations of the coupled external cavity semiconductor laser system. We therefore shall first discuss the dependence of the characteristic oscillation frequency of the tilting angle.

3) External Cavity Relaxation Oscillation and Frequency Locking: The characteristic frequency for the relaxation of the laser emission to its equilibrium value after an intermittent burst depends on tilting of the external cavity mirror. Fig. 4 shows the variation of this relaxation frequency plotted against the tilting angle. The marked points are the experimentally observed

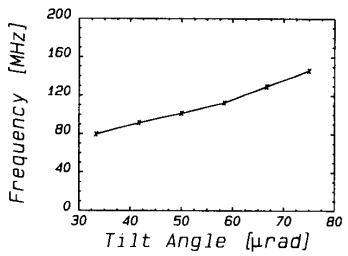

Fig. 4. Frequency of the external cavity semiconductor laser relaxation oscillations versus the horizontal tilting angle of the external cavity mirror. The marked points are the experimental data. The lines are connections between the experimental points as a guide for the eye.

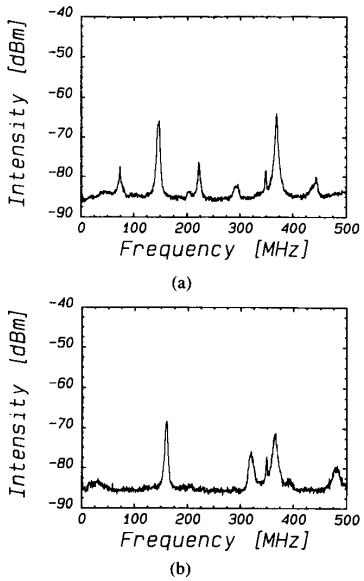

Fig. 5. (a) power spectrum corresponding to a horizonal tilting angle of 67 μrad. The ratio of the characteristic oscillation frequency with respect to the external cavity frequency is 2/5. (b) power spectrum corresponding to a horizontal tilting angle of 73 μrad.

frequencies, the lines between the points are linear interpolations as a guide for the eye. The frequency of the characteristic oscillation is shifted from $\sim\frac{1}{4}$ up to $\frac{1}{2}$ of the external cavity frequency with an increase of the mirror angle from 30 to 79 μrad. The noise in the power spectrum disappears between 30 and 60 μrad. For larger tilting between 60 and 79 μrad we observe pronounced sharp peaks in the power spectrum. Fig. 5 shows two typical power spectra exhibiting these sharp frequencies, Fig. 5(a) for 67 μrad and Fig. 5(b) for 73 μrad. In both sets of data the peak at 369 MHz corresponds to the lasing external cavity modes. In Fig. 5(a) the peak at 148 MHz is the characteristic oscillation frequency, in Fig. 5(b) the peak is at 155 MHz. Further peaks are caused by higher harmonics or by beat frequencies of the characteristic frequency with the external cavity modes. A very interesting feature to point out in Fig. 5(a) is the observation of a rational ratio of $\frac{2}{5}$ for the value of the frequency of the characteristic oscillation and the external cavity lasing frequency.

The minimum in the emitted light intensity is reached with a tilting angle of 79 μrad. Here we observe a characteristic relaxation oscillation frequency of about $\frac{1}{2}$ of the external cavity frequency. With further increase of the tilting angle of the external cavity mirror in the horizontal direction, the light intensity increases again and the characteristic oscillation disappears.

The identification of the characteristic oscillation as the intrinsic relaxation oscillation of the external cavity laser will be given in Section IV of this paper where the theoretical predictions for the relaxation oscillations are applied to these experimental data.

4) Side Maximum: Now we discuss the tilting regime where a pronounced side maximum is observed. This side maximum appears for a horizontal mirror tilting larger than 79 μrad (compare Fig. 2). In this regime no relaxation oscillations are observed. In Fig. 6 we show a power spectrum for an angle of 83 μrad. The characteristic oscillation frequency at 360 MHz has nearly completely disappeared and we observe the low-frequency noise again. The behavior in the side maximum region is similar to regime 2) with respect to intermittency and low-frequency noise behavior. The same phenomena has been observed by Park *et al.* [16]. The origin of the side maximum has been explained as a positive interference effect of the feedback light with the emitted light.

5) Double External Cavity Round-Trip: Now we discuss the regime of tilting angles of the external cavity mirror where the double round-trip frequency replaces the single round-trip frequency. This phenomen appears for tilting angles of external cavity mirror larger than approximately 200 μrad in horizontal direction as well as in vertical direction. In this case the light intensity is reflected once at the facet of the semiconductor laser before it reenters the active region of the semiconductor laser as reported by Park *et al.* in [12]. This means that the light is propagating twice through the external cavity before reentering into the laser.

In Section II-A we have followed a horizontal tilting path. Now in Section II-B we discuss a vertical tilting path to give a complete overview of the titling behavior.

B. Vertical Tilting of the External Cavity Mirror

The observation of regime 1), 2), 4) and 5) is not restricted to horizontal mirror tiltings. We achieve the same results for vertical mirror tiltings, only the tilting angles are a little different. However, regime (4) does not appear in the case of vertical tilting (compare Fig. 2). In this case regime 3) is directly followed by regime 5) without observation of regime 4). This reflects the asymmetry of the geometric structure of the active region of the semiconductor laser. The width of the active region is about one order of magnitude larger than its height. Therefore the angle where the side maximum would occur for vertical tiltings is larger than the angle where the double external cavity round-trip occurs.

Now, we compare the observations for horizontal and vertical tilting of the external cavity mirror. The parameter to classify the behavior of laser output is the light intensity. The output behavior of the laser remains the same following a contour line for constant light intensity in Fig. 2(b). As we will see in Section III, this means that the characteristic oscillation frequency which determines the instable behavior in regime 3) remains constant following a contour line.

The differences in the behavior for horizontal and vertical tilting can be attributed to the different lateral and transversal

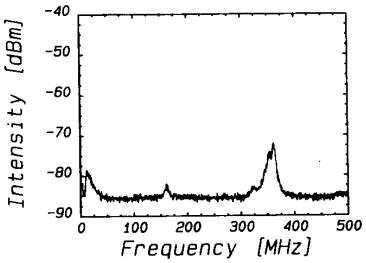

Fig. 6. Power spectrum for a horizontal tilting angle (83 μrad) corresponding to the transition region from the minimum in the output power to the side maximum. The external cavity laser characteristic oscillation frequency has nearly disappeared and the low-frequency noise increases again.

extension of the active region of the semiconductor laser. Therefore the angles, where the regimes appear, are different for horizontal and vertical tilting and this is the reason that regime 4) does not appear for the vertical tilting direction.

In the following section of the present paper we discuss theoretically the external cavity laser relaxation oscillation frequency on the base of the model proposed by Land and Kobayashi [17].

III. Model

In order to explain our experimental findings theoretically, we start with the model which was first proposed by Lang and Kobayashi [17] and continued by several groups [12], [16], [18]–[23]. In this method the electric field density $\mathfrak{E}$ and the carrier density N are described by two nonlinear nonautonomous differential equations:

$$\dot{\mathfrak{E}} = [i\omega(N) + \tfrac{1}{2}[G(N) - \Gamma]] \cdot \mathfrak{E}(t) + \kappa \cdot \mathfrak{E}(t - \tau) \quad (1)$$

$$\dot{N} = J - \gamma \cdot N - G(N) \cdot |\mathfrak{E}(t)|^2 \quad (2)$$

where the symbols have the following meanings:

$\omega(N)$	eigenfrequency of the semiconductor laser,
$G(N)$	optical gain function,
Γ	electric field decay rate,
κ	feedback rate,
J	electrical pumping rate,
γ	carrier density decay rate, and

$\mathfrak{E}$ and N are the electric field and the carrier density, respectively. With the usual ansatz

$$\mathfrak{E}(t) = E(t) \cdot \exp[i\omega_0 + i\varphi(t)]. \quad (3)$$

we split the electric field density into amplitude E and phase φ. We then obtain the characteristic equation for the eigenvalues.

$$D(\lambda) = 0 \quad (4)$$

by small-signal analysis around the equilibrium values of the solitary semiconductor laser. $D(\lambda)$ in (4) is defined via

$$\begin{aligned} D(\lambda) = {} & \lambda^3 - \lambda^2 \cdot [\Gamma_R + 2(\kappa \cdot \Delta\tau) \cdot \cos \omega_0\tau] \\ & + \lambda \cdot [(\kappa \cdot \Delta\tau)^2 + 2\Gamma_R \cdot (\kappa \cdot \Delta\tau) \\ & \cdot \cos \omega_0\tau + \omega_R^2] \\ & - \Gamma_R \cdot (\kappa \cdot \Delta\tau)^2 - \omega_R^2 \cdot (\kappa \cdot \Delta\tau) \\ & \cdot [\cos \omega_0\tau - \alpha \cdot \sin \omega_0\tau]. \end{aligned} \quad (5)$$

The symbols have the following meanings:

$\Delta\tau = 1 - \exp(\lambda\tau)$	(6)
$\omega_R^2 = \Gamma \cdot G_N \cdot E_0^2$	square of the relaxation oscillation frequency of solitary semiconductor laser, (7)
$\Gamma_R = \gamma + G_N \cdot E_0^2$	relaxation rate of the solitary semiconductor laser, (8)
$G_N = \partial G/\partial N$	differential optical gain,
E_0	equilibrium value of the electric field density amplitude,
ω_0	equilibrium value of the frequency of the laser light,
$\alpha = 2 \cdot (\partial\omega/\partial N)/(\partial G/\partial N)$	linewidth enhancement factor.

In our case injection current is chosen to be in the region above the threshold with feedback but below the value which is required for the coherence collapse. In this region we can expect that the laser is determined by the eigenfrequencies of the external cavity. Therefore we can set $\omega_0\tau \simeq 2\pi \cdot n$ ($n \in \mathbb{N}$). Furthermore, we assume that the observed frequencies are nearly undamped and close to the eigenfrequencies of the external cavity. This results in $\Delta\tau \simeq -\lambda\tau$ for (6). Inserting these assumptions into (4) yields for the imaginary part of λ:

$$\mathrm{IM}(\lambda)^2 = \omega_{ER}^2 = \frac{\omega_R^2}{1 + \kappa\tau} - \frac{1}{4} \cdot \Gamma_R^2. \quad (9)$$

Equation (9) is very similar to the formula obtained by Fujiwara *et al.* [14]. However, different to Fujiwara *et al.* we have taken into account the damping term because the damping enters into the magnitude of the relaxation frequency. Equation (9) can now be easily interpreted. In the case of no feedback ($\kappa = 0$) the well-known formula for the relaxation oscillation frequency is obtained. However, with feedback this frequency becomes renormalized by the product of the feedback level and the delay time of the external cavity. Inserting the expressions for ω_R^2 and Γ_R^2 into (9) yields a quadratic equation for ω_{ER}^2 in terms of the observed light intensity $I_0 = E_0^2$.

$$\begin{aligned} \omega_{ER}^2 = {} & -\frac{1}{4} G_N^2 \cdot I_0^2 + \left[\frac{1}{1 + \kappa\tau} - \frac{1}{2}\frac{\gamma}{\Gamma}\right] \\ & \cdot \Gamma \cdot G_N \cdot I_0 - \frac{1}{4}\gamma^2. \end{aligned} \quad (10)$$

The renormalized relaxation oscillation frequency of the external cavity semiconductor laser ω_{ER}^2 depends parabolically on the light intensity I_0. We would like to point out that this behavior is markedly different from the behavior of the solitary semiconductor laser. For the solitary laser κ is equal to zero. Consequently, in (9) the term with ω_R^2 is larger by several orders of magnitude than the term with Γ_R^2. This results in the well-known linear relation (7) between the square of the relaxation oscillation frequency and the light intensity. In the case of strong feedback the term with ω_R^2 is no more dominant compared to Γ_R^2.

In the following chapter we compare this model with the results of two set of experiments.

IV. Comparison with Experimental Results

We now compare the model with our experimental results. First we consider experiments where the tilting angle of the external cavity mirror is kept constant and the injection current is

changed. In the second type of experiment the injection current is kept constant and the tilting angle is changed. In particular we will show that we are able to identify the characteristic oscillation frequencies observed so far as the relaxation oscillations of the coupled system.

A. Constant Mirror Tilting

In the first set of experiments, we have tilted the external cavity mirror until regime 3) is reached and the external cavity laser characteristic oscillation frequency have been observed. Then we increase the injection current and determine the frequency of the characteristic oscillations with the RF spectrum analyzer. The marked points in Fig. 7 are the square of the observed frequencies plotted versus the time-averaged light intensity. The curve in Fig. 7 is fitted to the experimental data according to (10). A very good fit is obtained, which proves that the characteristic oscillation in fact corresponds to the relaxation oscillation of the coupled cavity laser. As a result of the fit we obtain the values for the differential gain $G_N = 2.441 \cdot 10^{-6}\ s^{-1}\ cm^3$ and the carrier relaxation rate $\gamma = 4.043 \cdot 10^8\ s^{-1}$ corresponding to an electronic lifetime of $\tau_E = 2.474$ ns.

Comparing the fitted curve with the experimental data in Fig. 7 we find reproducible flat plateaus in the experimental data for some frequencies, whereas these plateaus are absent in the calculated curve. These plateaus in Fig. 7 are indicated with fractions corresponding to a locking of the relaxation oscillation frequency in rational ratios with respect to the lasing external cavity frequency. These steps obviously correspond to frequency locked states where the relaxation oscillation period is locked to the external cavity frequency. This is the same phenomena as shown in Fig. 5(a) and discussed in Section III-A-3. In Fig. 7 the most pronounced plateau corresponds to a locking ratio of $\frac{1}{3}$. The next clear step corresponds to a locking ratio of $\frac{3}{8}$. Furthermore, we can identify the locking ratio of $\frac{2}{5}$ and $\frac{2}{7}$ between the external cavity frequencies and the relaxation oscillation frequency. The observed steps give indications that the locking ratios follow the hierarchy of the Farey tree.

B. Constant Injection Current

In the second set of experiments, we have kept the injection current constant at 51.6 mA, which is between the threshold value of the external cavity laser and the value where the coherence collapse is observed. We then have tilted the external cavity mirror until regime (3) is reached where the external cavity relaxation oscillations are observed (cf. the data of Section II-A-3). A quantitative discussion of the data requires the knowledge of the feedback rate κ. This quantity, however is not directly measurable, because of the uncertainty of the coupling losses. We therefore have used the averaged light intensity as a measure of the feedback rate. We obtain the feedback rate as a function of light intensity by the stationary solution of the rate equations [(1) and (2)]. As a result, we find the following relation between the feedback rate and the average light intensity (for injection currents between the threshold values with and without feedback):

$$\kappa = \frac{1}{2} \cdot \frac{\Gamma}{\gamma} \cdot G_N \cdot I. \tag{11}$$

Inserting (11) into (10) yields a relation between the light intensity and the relaxation oscillation frequency with only an implicit dependence on the feedback rate κ. In our experimental results we have found a relation between the light intensity and

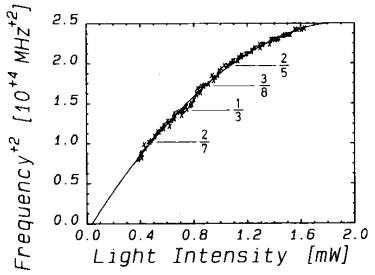

Fig. 7. Square of the relaxation oscillations (ω_{ER}^2) versus light intensity. The points represent the measured values of frequency and light intensity corresponding to one fixed tilting and different values of the injection current. The full line represents a fit to the data points according to (10). Deviations (plateaus) between the calculated curve and the data points are attributed to frequency locked states which fractions are indicated in the figure by the ratio of the two frequencies.

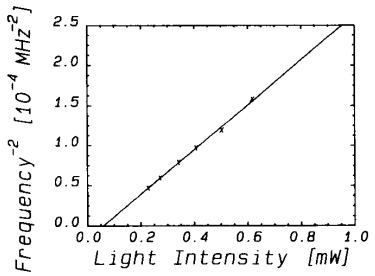

Fig. 8. Square of the relaxation oscillations (ω_{ER}^2) versus light intensity. The points represent the measured values of the relaxation frequency and the emitted intensity corresponding to different tilting angles at fixed injection current. The full line represents a fit through the data according to (12).

the relaxation oscillation frequency with a power of -0.54. In order to compare with these results, we expand the equation for ω_{ER}^{-2} and obtain, neglecting higher order terms:

$$\omega_{ER}^{-2} \simeq \frac{-1}{\gamma \cdot (\frac{1}{4}\gamma - 2/\tau)} + \frac{G_N}{\gamma \cdot (\frac{1}{4}\gamma - 2/\tau)^2} \cdot I_0. \tag{12}$$

We have plotted ω_{ER}^{-2} versus the light intensity in Fig. 8. The marked points are the experimental data for different tilting angles of the external cavity mirror. The solid curve is fitted to the data points according to (12). We obtain $G_N = 9.992 \cdot 10^{-6}\ s^{-1}\ cm^3$ for the differential gain and $\gamma = 4.800 \cdot 10^9\ s^{-1}$ for the carrier relaxation rate by the analysis of the fit parameters. These values are slightly different from the values determined from the variation of ω_{ER} with the injection current in the first type of experiment (Section IV-A). However, both values are within the accuracy of the independently determined parameters. We therefore conclude that the dynamics of the external cavity semiconductor laser is determined by the relaxation oscillations of the coupled laser system. The relaxation oscillation frequency acts as an internal clock which determines the distribution of intermittencies in the unstable regime and sets a lower limit for the time interval between intermittent breakdowns of the light intensity.

V. Conclusion

We have investigated the behavior of semiconductor lasers with external feedback under variable feedback conditions. We

have classified the behavior of the light output into five regions according to the tilting angle (misalignment) of the external cavity mirror. We have shown the appearance of an intermittent instability in the originally stable regime of the external cavity laser, caused by the tilting of the external cavity mirror. The rate of the break downs of the light intensity is directly related to the relaxation oscillation frequency of the external cavity semiconductor laser. The observed increase of the relaxation oscillation frequency with an increase of the tilting angle is related to the decrease of the external cavity Q value. We have described the experimental observations by a theoretical model based on the coupled nonlinear rate equations for the electric field density $\mathfrak{E}$ and the carrier density N which allows a physical interpretation of the experiment. However, the model cannot explain the microscopic origin of the instability. Therefore noise terms should be included into the rate equation model for a complete description of our experimental findings.

ACKNOWLEDGMENT

We are very grateful to J. G. McInerney, J.-D. Park, D.-S. Seo, and R. Nietzke for helpful discussions.

REFERENCES

[1] R. F. Kazarinov and C. H. Henry, "The relation of line narrowing and chirp reduction resulting from the coupling of a semiconductor laser to a passive resonator," *IEEE J. Quantum Electron*, vol. QE-23, pp. 1401-1409, Sept. 1987.

[2] J. P. van der Ziel, "Modelocking of semiconductor lasers," in *Semiconductors and Semimetals*, R. K. Willardson and A. C. Beer, Eds. Orlando, FL: Academic, 1985, pp. 1-68.

[3] T. Mukai and K. Otsuka, "New route to optical chaos: Successive-subharmonic-oscillation cascade in a semiconductor laser coupled to an external cavity," *Phys. Rev. Lett.*, vol. 55, pp. 1711-1714, Oct. 1985.

[4] C. H. Henry and R. F. Kazarinov, "Instability of semiconductor lasers due to optical feedback from distant reflectors," *IEEE J. Quantum Electron.*, vol. QE-22, pp. 294-301, Feb. 1986.

[5] Y. Cho and T. Umeda, "Observation of chaos in a semiconductor laser with delayed feedback," *Opt. Commun.*, vol. 59, pp. 131-136, Aug. 1986.

[6] R. W. Tkach and A. R. Chraplyvy, "Regimes of feedback effects in 1.5-μm distributed feedback lasers," *J. Lightwave Technol.*, vol. LT-4, pp. 1655-1661, Nov. 1986.

[7] P. Glas, R. Müller, and G. Wallis, "Determination of power spectra and attractor dimensions for a GaAlAs laser with external feedback," *Opt. Commun.*, vol. 68, pp. 133-138, Sept. 1988.

[8] G. C. Dente, P. S. Durkin, K. A. Wilson, and C. E. Moeller, "Chaos in the coherence collapse of semiconductor lasers," *IEEE J. Quantum Electron.*, vol. 24, pp. 2441-2447, Dec. 1988.

[9] J. Sacher, W. Elsässer, and E. O. Göbel, "Intermittency in the coherence collapse of a semiconductor laser with external feedback," *Phys. Rev. Lett.*, vol. 63, pp. 2224-2227, Nov. 1989.

[10] The models [(1) and (2)] contain a delay term $\mathfrak{E}(t - \tau)$ which leads directly to a infinite dimensional system.

[11] J. Mørk, "Nonlinear dynamics and stochastic behavior of semiconductor lasers with optical feedback," Ph.D dissertation, The Technical University of Denmark, Denmark, Aug. 1988.

[12] J. D. Park, D. S. Seo, J. G. McInerney, G. C. Dente, and M. Osiński, "Low-frequency self-pulsations in assymetric external cavity semiconductor lasers due to multible feedback effects," *Opt. Lett.*, vol. 14, pp. 1054-1056, Oct. 1989.

[13] K. Vahala, C. Harder, and A. Yariv, "Observation of relaxation resonance effects in the field spectrum of semiconductor lasers," *Appl. Phys. Lett.*, vol. 42, pp. 211-213, Feb. 1983.

[14] M. Fujiwara, K. Kubota, and R. Lang, "Low-frequency intensity fluctuations in laser diodes with external optical feedback," *Appl. Phys. Lett.*, vol. 38, pp. 217-220, Feb. 1981.

[15] K. Tatah and E. Garmire, "Low-frequency intensity noise resonance in an external cavity GaAs laser for possible laser characterization," *IEEE J. Quantum Electron.*, vol. 25, pp. 1800-1807, Aug. 1989.

[16] D. S. Seo, J. D. Park, J. G. McInerney, and M. Osiński, "Multible feedback effects in asymetric external cavity semiconductor lasers," *IEEE J. Quantum Electron.*, vol. 25, pp. 2229-2238, Nov. 1989.

[17] R. Lang and K. Kobayashi, "External optical feedback effects on semiconductor injection laser properties," *IEEE J. Quantum Electron.*, vol. QE-16, pp. 347-355, Mar. 1980.

[18] B. Tromborg, J. H. Osmundsen, and H. Olesen, "Stability analysis for a semiconductor laser in an external cavity," *IEEE J. Quantum Electron.*, vol. QE-20, pp. 1023-1032, Sept. 1984.

[19] H. Olesen, J. H. Osmundsen, and B. Tromborg, "Nonlinear dynamics and spectral behavior for an external cavity laser," *IEEE J. Quantum Electron.*, vol. QE-22, pp. 762-773, June 1986.

[20] J. Mørk, B. Tromborg, and P. L. Christiansen, "Bistability and low-frequency fluctuations in semiconductor lasers with optical feedback: A theoretical analysis," *IEEE J. Quantum Electron.*, vol. 24, pp. 123-133, Feb. 1988.

[21] G. A. Acket, D. Lenstra, A. J. den Boef, and B. H. Verbeek, "The influence of feedback intensity on longitudinal mode properties and optical noise in index-guided semiconductor lasers," *IEEE J. Quantum Electron.*, vol. QE-20, pp. 1163-1169, Oct. 1984.

[22] D. Lenstra, B. H. Verbeek, and A. J. den Boef, "Coherence collapse in single-mode semiconductor lasers due to optical feedback," *IEEE J. Quantum Electron.*, vol. QE-21, pp. 674-679, June 1985.

[23] J. Cohen, R. R. Drenten, and B. H. Verbeek, "The effect of optical feedback on the relaxation oscillation in semiconductor lasers," *IEEE J. Quantum Electron.*, vol. QE-21, pp. 1989-1995, June 1985.

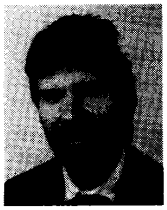

Joachim Sacher was born in Koblenz, Germany, on November 8, 1962. He received the Diploma degree in physics from the Philipps-Universität Marburg, Marburg, Germany, in 1988.

His main research interests include the nonlinear dynamical behavior and mode locking of semiconductor lasers.

Mr. Sacher is member of the German Physical Society.

Wolfgang Elsässer was born in Pforzheim, West Germany, on September 29, 1954. He received the Dipl. Phys. degree from the University of Karlruhe, Karlsruhe, West Germany, in 1980 and the Ph.D. degree in physics from the University of Stuttgart, Stuttgart, West Germany, in 1984.

From 1981 to 1985, he was with the Max-Planck-Institut für Festkörperforschung, Stuttgart, working on the spectral and coherence properties of semiconductor lasers. In 1985, he joined the Philipps-Universität Marburg, Marburg, West Germany, where he is now engaged in the research on nonlinear optics instabilities and chaos, and mode locking, all with a primary focus on semiconductor lasers.

Dr. Elsässer is a member of the Germany Physical Society.

Ernst O. Göbel was born in Seelbach, West Germany, on March 24, 1946. He received the Diploma degree in physics from the University of Frankfurt am Main, West Germany, in 1970, and the Ph.D. degree in physics from the University of Stuttgart, Stuttgart, West Germany, in 1973.

In 1975 he was a Guest Scientist at Bell Laboratories, Holmdel, NJ, on a research fellowship from the Deutsche Forschungsgemeinschaft. From 1976 to 1980, he was with the University of Stuttgart working on semiconductor lasers and high-excitation phenomena in semiconductors. In 1980 he joined the Max-Planck-Institut für Festkörperforschung, Stuttgart, where he was engaged in research on picosecond and femtosecond phenomena in solids, picosecond optoelectronics, and semiconductor lasers. He is presently continuing this work as a Full Professor at the Philipps-Universität Marburg, Marburg, Germany.